ISSN : 0974 - 7494 Volume 6 Issue 4

Trade Science Inc.

Nano Science and Nano Technology

An Indian Journal

Full Paper

NSNTAIJ, 6(4), 2012 [151-158]

On the corrosion behaviour of Al/SiC and Al/Al_2O_3 metal matrix nanocomposites

T.S.Mahmoud*, E.Y.E-lkady, A.Al-Shihri

King Khalid University (KKU), Abha, Kingdom of Saudi Arabia, (KSA)

Received: 30th March, 2012 ; Accepted: 3rd September, 2012

ABSTRACT

The present investigation studies of the static immersion corrosion behavior of Al/Al_2O_3 and Al/SiC nanocomposites in 1 M HCl solution. The aforementioned nanocomposites were fabricated using conventional powder metallurgy (P/M) route. The effect of nanoparticles size and volume fraction on the corrosion behavior of nanocomposites was studied. The durations of the corrosion tests ranged from 24 to 120 hours and the temperature of the solution ranged from ambient to 75 °C. The corrosion rates of the nanocomposites were calculated using the weight loss method. The results showed that Al/SiC and Al/ Al/Al_2O_3 MMNCs exhibited lower corrosion rates than the pure Al matrix. Such behavior was noticed at both room temperature and higher temperatures. Generally, the Al/Al_2O_3 nanocomposites exhibited lower corrosion rates than the Al/SiC nanocomposites. The Al/ Al/Al_2O_3 containing (60 nm) exhibited the higher corrosion resistance among all the investigated nanocomposites. The corrosion rate was reduced with the increase the exposure time and the volume fraction of the nanoparticles. While it increased with increasing the nanoparticles size and the solution temperature.

KEYWORDS

Nanocomposites;
Corrosion;
Aluminum alloys;
Powder metallurgy.

INTRODUCTION

Aluminium-based metal matrix composites (MMCs) become attractive for the automotive and aerospace industries when a lightweight and near-net-shape component is desired. Aluminum-based MMCs are well known for their high wear resistance, improved tensile and fatigue strengths at elevated temperatures[1]. The mechanical and tribological characteristics of MMCs were extensively studied, while corrosion characteristics are of increasing importance as MMCs become candidates for use in specific components subjected to corrosive media. Generally, the corrosion resistance of aluminium-based MMCs is less than the monolithic alloys, due to several reasons such as the crevices at the matrix/reinforcement interface, manufacturing defects, internal stress, microstructural differences and galvanic effects due to coupling of the matrix and reinforcement[2-4].

Recently, metal matrix nanocomposites (MMNCs) have become more attractive in various applications because of their improved mechanical properties over conventional micro-particle reinforced MMCs. These materials are expected to exhibit good corrosion resistance in the aggressive environments. Therefore, determination of the corrosion resistance of composite materials reinforced with nanoceramic additives is very important. Most studies conducted on Al matrix nanocomposites, have been focused on the corrosion susceptibility in NaCl solutions[5,6]. For example, *El-Mahallawi et al.*[5] studied the corrosion behavior in 3.5% NaCl solution of A356 Al alloy reinforced with nano-Al_2O_3 particulates. The results showed that the A356 the monolithic alloy exhibited high corrosion rates when compared with the nanocomposites. *Durai et al.*[6] studied effect of mechanical milling on the corrosion behavior of Al–Zn/Al_2O_3 composite in NaCl solution. Results of the corrosion tests, evaluated using the potentiodynamic method, indicate that corrosion of the investigated composite materials depends on the weight fraction of the reinforcing particles. The milled composite material Al–Zn/Al_2O_{3p} has higher corrosion resistance in the selected environment compared to unmilled composite Al–Zn/Al_2O_{3p}.

Literature regarding the corrosion behavior of Al matrix nanocomposites in acidic media is limited. Accordingly, the aim of the current investigation is to study the static immersion corrosion characteristics of Al/SiC and Al/Al_2O_3 nanocomposites in 1 M HCl solution. Several nanocomposites containing different sizes and volume fractions of SiC and Al_2O_3 nanoparticulates were prepared using conventional powder metallurgy (P/M) route. Both the pure Al matrix and the nanocomposites were subjected to identical corrosion test conditions to study the influence of the material parameters (such as the nanoparticles type, size and volume fraction) as well as the corrosion test conditions (such as the solution temperature and exposure duration) on the corrosion behavior of the nanocomposites.

EXPERIMENTAL PROCEDUERS

In the current study, commercially pure Al powder having minimum purity of 99.7 % was used as a matrix material. The Al powders size ranged between 10 and 100 μm. Both of SiC and Al_2O_3ceramic nanoparticulates were used as reinforcing agents. Each of SiC and Al_2O_3 nanoparticulates has two different average sizes, typically, 200 nm and 60 nm.

Several Al-based nanocomposites containing up to 5 vol.-% of SiC and Al_2O_3 nanoparticulates were prepared using conventional powder metallurgy (P/M) route as follows: Both Al powder and nanoparticles in addition to 0.5-1.5 wt.-% paraffin lubricant wax were placed into a blender, mechanically mixed until a homogeneous mixture is achieved, and then placed into containers. The mixed Al/nanoparticles powders were cold compacted in a tool steel die shown schematically in Figure 1. The powders were then pressed using a hydraulic press having a capacity of 400 kN. The applied compaction pressure during compaction was about 500 MPa. The nanocomposites produced from the cold compaction step were subjected to sintering at 600 °C for 100 min. The sintering process was performed under argon inert gas atmosphere. After sintering, the nanocomposites were subjected to hot extrusion. The nanocomposites billets were extruded at 500 °C using the extrusion die. The heating process was carried out using Ni-Cr coils around the upper cylinder. The extrusion reduction ratio was 2:1 by area. The final nanocomposite samples had cylindrical shape of 10 mm diameter and about 100 mm length.

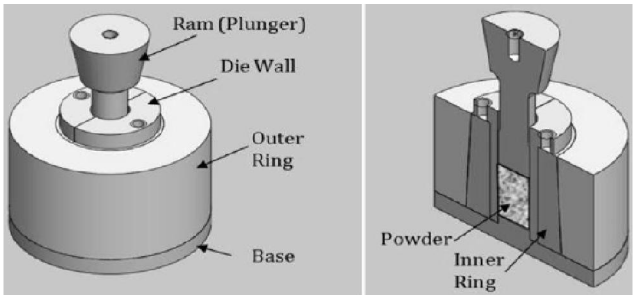

Figure 1 : A schematic illustration of the cold compaction die.

Samples from the extruded rods were cut in transverse directions (i.e. cross sectional) for microstructural examinations. Specimens were ground under water on a rotating disc using silicon carbide abrasive discs of increasing grade up to 1200 grit. Then they were polished using 10 μm alumina paste and 3 μm diamond paste Microstructural observations were conducted using optical and field emission scanning electron microscopes.

The corrosion tests were static immersion tests conducted at room temperature, 50 and 75 °C using the conventional weight loss method to an accuracy of 0.1 mg.

Each specimen was first weighed before being immersed in 100 ml of 1 M HCl solution and later taken out after 24, 48, 72, 96 and 120 hours respectively. After each corrosion test, the specimen was immersed in Clark's solution for 10 min and gently cleaned with a soft brush to remove adhered scales. Clark's solution is a standard mixture containing potassium chloride, potassium phthalate, potassium phosphate, boric acid and sodium hydroxide[7]. After drying thoroughly, the specimens were weighed again. The weight loss was measured and converted into corrosion rate expressed in mils penetration per year (mpy). The corroded surfaces were examined using field emission scanning electron microscopy (FEFESEM).

Corrosion tests were carried out according to by suspending the disc-shaped samples (10 mm diameter and about 5 mm thick) in a still solution of 1 M HCl. To avoid crevice corrosion, the specimens were suspended in the solution with a plastic string. The results of corrosion tests were evaluated using weight loss measurements, performed following the ASTM-G31 recommended practice[8]. Before immersing in 1 M HCl solution, disc-shaped specimens were ground to 1200 grit and then cleaned with deionized water followed by rinsing with methanol and dried. For the accelerated tests, a 1 M HCl solution was prepared, and heated to 50±2 and/or 75±2 æ%C using an electric heater. The specimens are put into the warm solution and a glass cover put on the top of the vessel to prevent evaporation.

RESULTS AND DISCUSSION

Microstructure of nanocomposites

Figure 2 shows typical optical micrographs of the fabricated Al/Al_2O_3 and Al/SiC nanocomposites. It has been found that the agglomeration percent of the nanoparticulates tends to increase when the volume fraction of the nanoparticulates dispersed into the Al matrix is increased. Such agglomerations were found to be concentrated on the grain boundaries of Al grains (see Figure 2c). The agglomerations size was found varying between 1 and 5 µm. Generally, it has been found that the Al/Al_2O_3 nanocomposites exhibited better nanoparticulates distributions than Al/SiC nanocomposites. The Al/SiC nanocomposites exhibited more agglomeration percent when compared with the Al/Al_2O_3 nanocomposites. The agglomerations size in Al/SiC nanocomposites was found to vary between 0.5 and 10 µm. It has been found that the average size of the Al grains in the nanocomposites was not signifi-

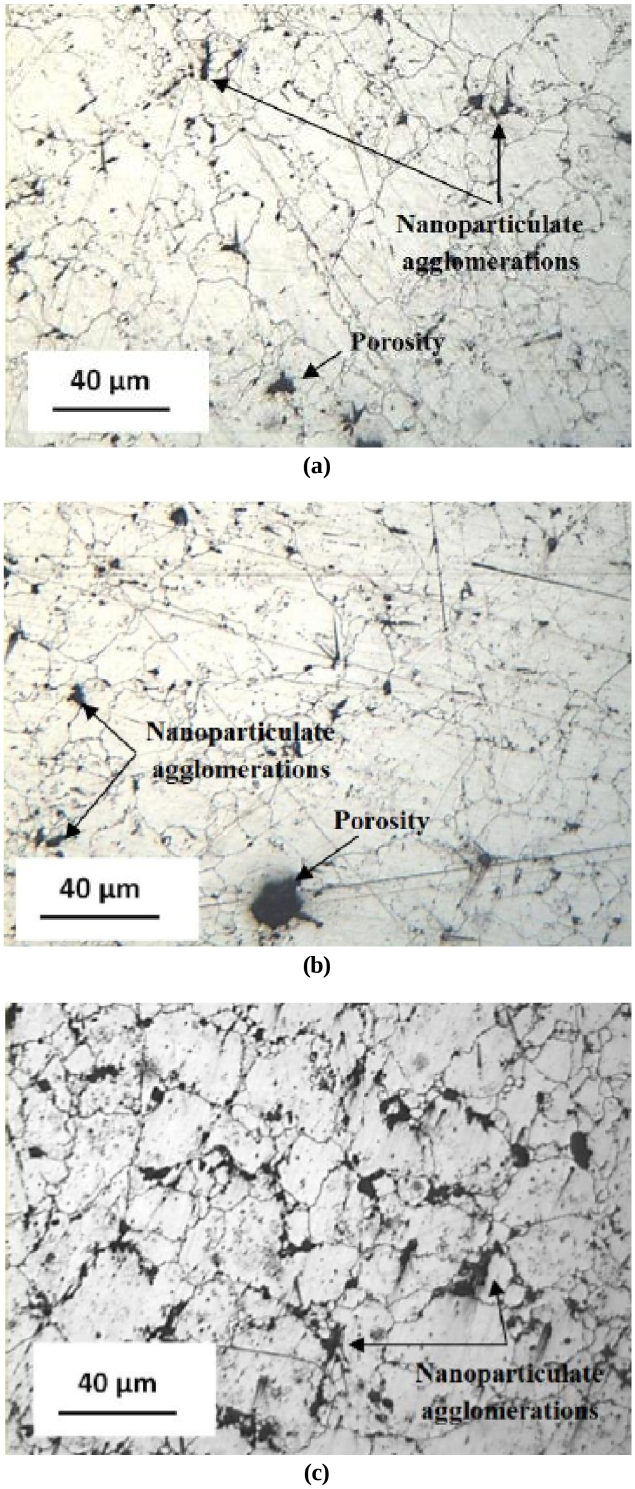

Figure 2 : Optical micrographs of (a) 3 vol.-% Al/Al_2O_3 (60 nm), (b) 5 vol.-% Al/Al_2O_3 (60 nm) and (c) 5 vol.-% Al/SiC (200 nm) nanocomposites.

cantly influenced by the volume fraction and/or the size of nanoparticulates.

Figure 3 shows typical FESEM micrographs for the investigated Al/Al$_2$O$_3$ and Al/SiC nanocomposites. It is clear that the nanoparticulates were successfully embedded in the Al matrix. According to the aforementioned results it can be concluded that the production of bulk nanocomposites using conventional P/M technique is effective. The SiC and Al$_2$O$_3$ nanoparticulates distribution in the Al matrix was fairly uniform. Although small agglomerates in Al/SiC and Al/Al$_2$O$_3$ nanocomposites still existed in the matrix, the agglomerates have been greatly improved when compared with the severe agglomerates in nanocomposites fabricated using traditional mechanical stirring method[9].

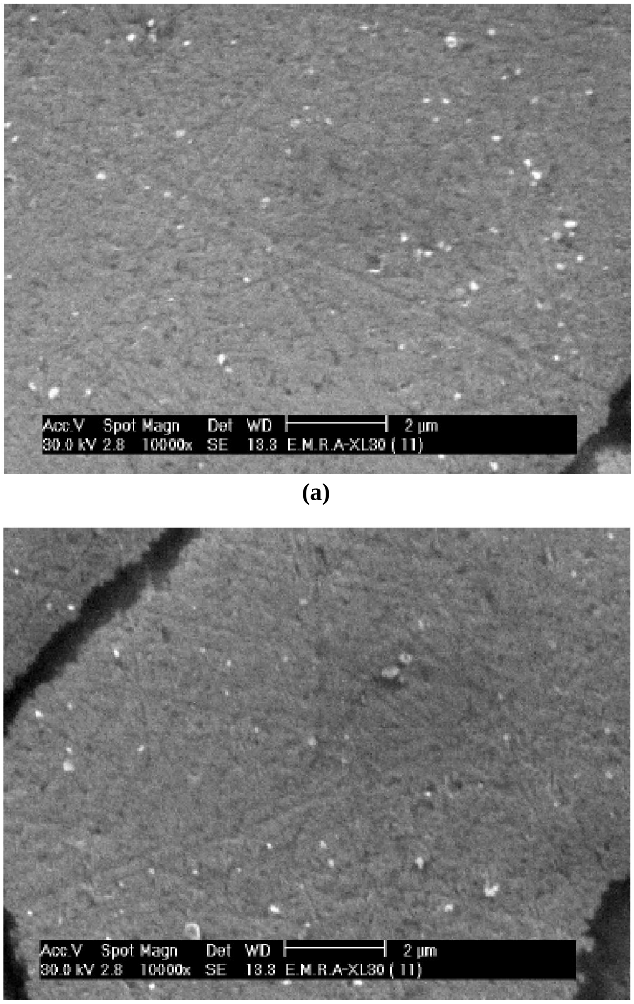

(a)

(b)

Figure 3 : FESEM micrographs of (a) Al/3 vol.-%Al$_2$O$_3$ nanocomposites (200 nm) and (b) Al/3 vol.-%SiC nanocomposites (200 nm).

Corrosion behaviour of nanocomposites at room temperature

Figure 4 shows the variation of the corrosion rate with the exposure time in 1 M HCl at room temperature of Al/Al$_2$O$_3$ and Al/SiC nanocomposite. It can be seen that in every case, there is a decrease in the corrosion rate with the increase in duration of exposure to the corrodent. Such observation implying that the corrosion resistance of the materials under investigation increases as the exposure time is increased. The phenomenon of decreasing the corrosion rate with respect to time indicates some passivation of the matrix alloy. For all the investigated materials, there is a trend of decreasing of the corrosion rate with the increase of the Al$_2$O$_3$ and SiC nanoparticles volume fraction. The pure Al matrix exhibited higher corrosion rate than the Al/Al$_2$O$_3$ and Al/SiC nanocomposites. Both SiC and Al$_2$O$_3$ nanoparticulates are ceramic materials and they remains inert and it is expected that they are unaffected by the acid medium during the corrosion tests. The results revealed that corrosion rate of the Al/SiC and Al/Al$_2$O$_3$ MMNCs was reduced by reducing the SiC and Al$_2$O$_3$ nanoparticles size. It has been found that the nanocomposites containing 60 nm of nanoparticulates have lower corrosion rates than the nanocomposites containing 200 nm of the nanoparticulates. Such notice was observed for both nanocomposites containing both SiC and Al$_2$O$_3$ nanoparticulates. Moreover, the nanocomposites containing Al$_2$O$_3$ nanoparticulates exhibited lower corrosion rates than the nanocomposites containing SiC nanoparticulates.

In this study it has been found that the Al matrix composites with nano-size SiC and Al$_2$O$_3$ reinforcements offer better corrosion resistance in 1 M HCl at room temperature than the pure Al matrix material. The matrix grain size is in the micrometer range. The corrosion behavior of nanocomposites depends on various factors such as the reinforcing nanoparticles type, their size and volume fraction.

Eeffect of temperature on the corrosion behaviour of nanocomposites

Figure 5 shows the variation of the corrosion rate of the Al/Al$_2$O$_3$ and Al/SiC nanocomposites with the temperature after exposure in 1 M HCl for 48 hours. It has been found that the nanocomposites have lower corrosion rates when compared with the pure Al matrix at elevated temperatures up to 75 °C. Corrosion rates of the pure Al as well as the nanocomposites were found to increase linearly with the temperature (see Figure 5). This effect may attributed to the increased diffusion rate of hydrogen with increase in temperature, as well as the activation energy of the acid solution which boots hydrogen evaluation[10]. It is apparent that for all the investigated materials, as in the room temperature tests, there is a trend of decreasing the corrosion rate with the increase in both the SiC and Al_2O_3 nanoparticles content. Moreover, it has been found that reducing the nanoparticles size from 200 nm to 60 nm reducing the corrosion rate at both 50 °C and 75 °C. The Al/Al_2O_3 nanocomposites exhibited lower corrosion rates than the Al/SiC nanocomposites. The Al/Al_2O_3 nanocomposites containing 5 vol.-% of Al_2O_3 nanoparticles having 60 nm exhibited the lowest corrosion rates among the investigated nanocomposites.

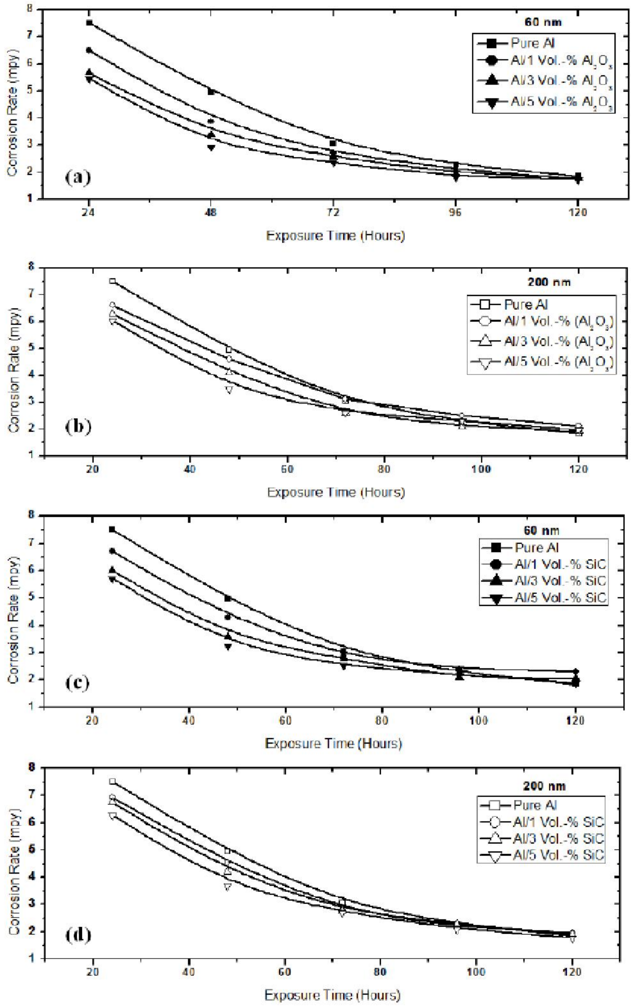

Figure 4 : Variation of the corrosion rate with the exposure time in 1 MHCl at room temperature for nanocomposites reinforced with (a) Al_2O_3 (60 nm); (b) Al_2O_3 (200 nm); (c) SiC (60 nm) and (d) SiC (200 nm) nanoparticulates.

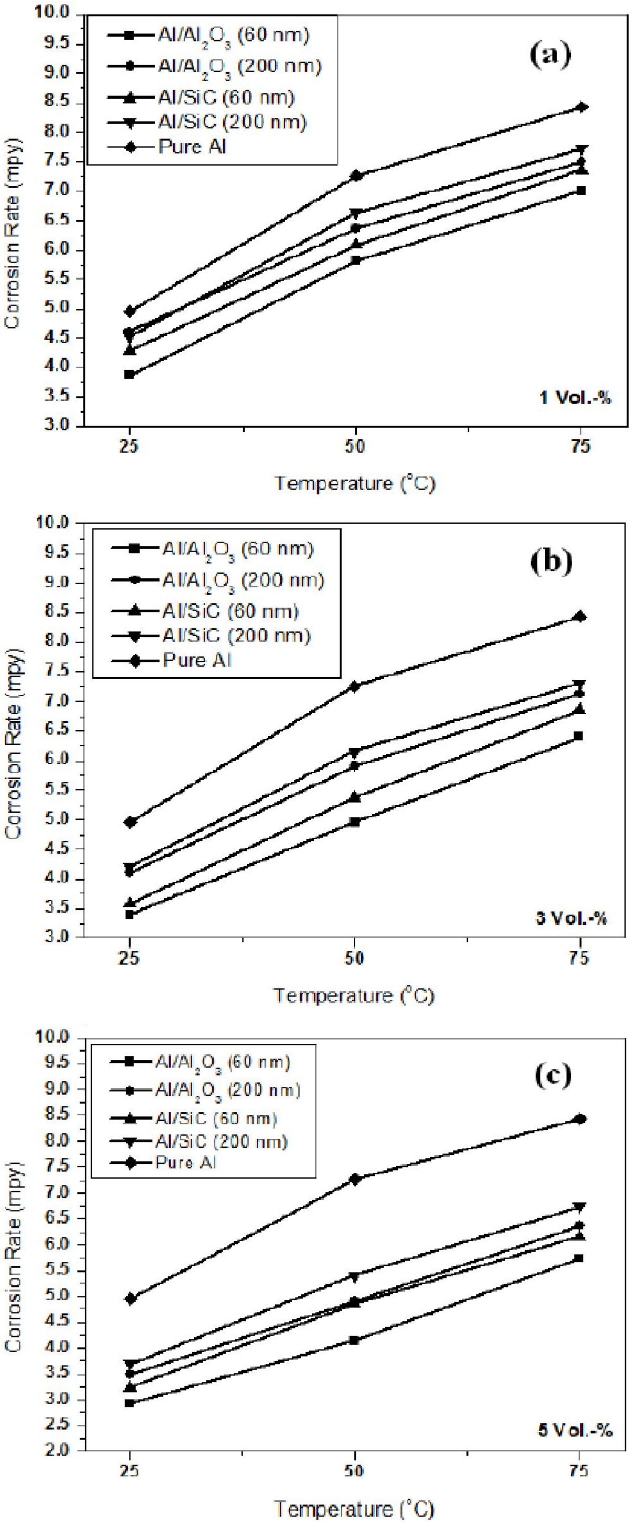

Figure 5 : Variation of the corrosion rates with temperature for Al/SiC and Al_2O_3 nanocomposites containing (a) 1 vol.-%, (b) 3 vol.-% and (c) 5 vol.-% of nanoparticulates having average size of 60 and 200 nm.

Corrosion morphology

Figure 6 shows typical FESEM micrographs of the corroded surfaces of pure Al matrix and Al/Al_2O_3 nanocomposites, containing 1 and 5 vol.-% of 60 nm Al_2O_3 particulates, after exposure for 96 hours in 1 M HCl solution at room temperature. It is clear that the surface of the pure Al was severely damaged, especially at the grain boundaries, when compared with the corroded surfaces of the Al/Al_2O_3 nanocomposites. Increasing the amount of Al_2O_3 nanoparticles from 1 to 5 vol.-% reduces the surface degradation (compare Figure 6b and 6c). In addition to grain boundary corrosion, pitting corrosion was observed in the pure Al matrix as well as the Al/Al_2O_3 and Al/SiC nanocomposites, especially those containing 1 vol-% of nanoparticulates. Figure 7 shows typical corrosion pitting occurred in 1 vol.-% Al/Al_2O_3 (60 nm) nanocomposites. Increasing the nanoparticulates content reduces the number of pits.

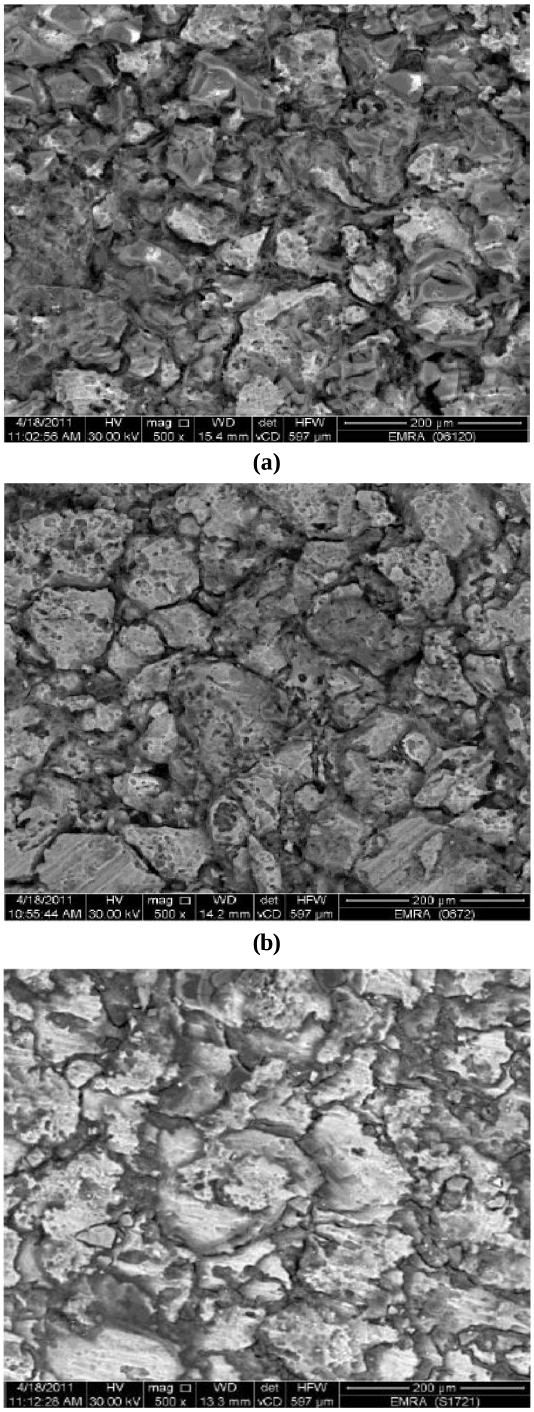

(a)

(b)

(c)

Figure 6 : FESEM micrographs of the corroded surfaces of (a) pure Al matrix, (b) and (c) 1 and 5 vol.-% (60 nm) Al/Al_2O_3 nanocomposites after exposure for 96 hours in 1 M HCl solution at room temperature.

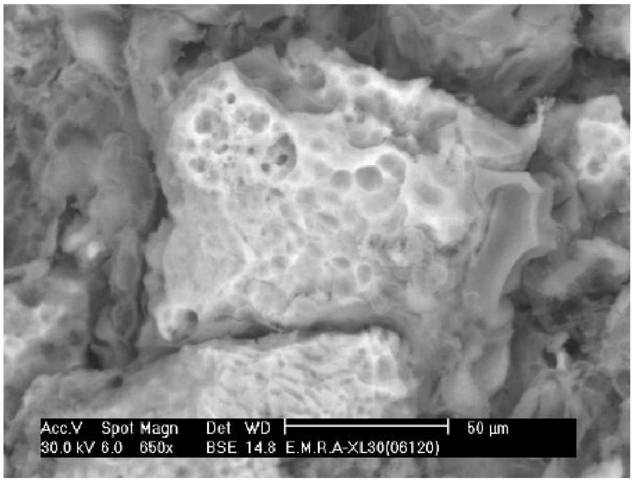

Figure 7 : FESEM micrograph shows the pitting corrosion occurred in 1 vol.-% Al/Al_2O_3 (60 nm) nanocomposites after exposure for 96 hours in 1 M HCl solution at room temperature.

Typical FESEM micrographs of the corroded surfaces of Al/SiC nanocomposites containing 1 vol.-% of 200 nm SiC nanoparticles after exposure in 1 M HCl solution for 96 hr at 50 and 75 °C are shown in Figure 8. It is clear that the amount of surface degradation increased with temperature. Surface crack were observed on the corroded surfaces at both 50 and 75 °C. The cracks were seen to develop along the grain boundaries. The size and depth of the crack were found to increase with both the exposure duration and temperature. Figure 9 shows example high magnification FESEM micrographs at the grain boundaries of the corroded surface of Al/SiC nanocomposite specimens containing 1 vol.-% of 60 nm and 200 nm SiC nanoparticulates. The specimen was exposed to 1 M HCl solution at 50 °C for 96 hr. It has been found that the SiC nanoparticles exist at the grain boundaries of the Al grains. Figure 10 shows EDX analysis of some SiC nanoparticles located at the grain boundaries. It is important to mention that it was difficult to verify the SiC nanoparticles from the FESEM micrographs only because of the low percentage and small size of SiC in the Al matrix.

The improvement of the corrosion resistance of the Al pure matrix found in the current investigation may attributed to the fact that both SiC and Al_2O_3 are being ceramics and remain inert in the acid. They are hardly affected by the acidic medium. Though the corrosion rate is lesser than that of the matrix metal, the nanocomposites also showed the formation of pits on the surface. The number of pits gets decreased with the addition of SiC and Al_2O_3

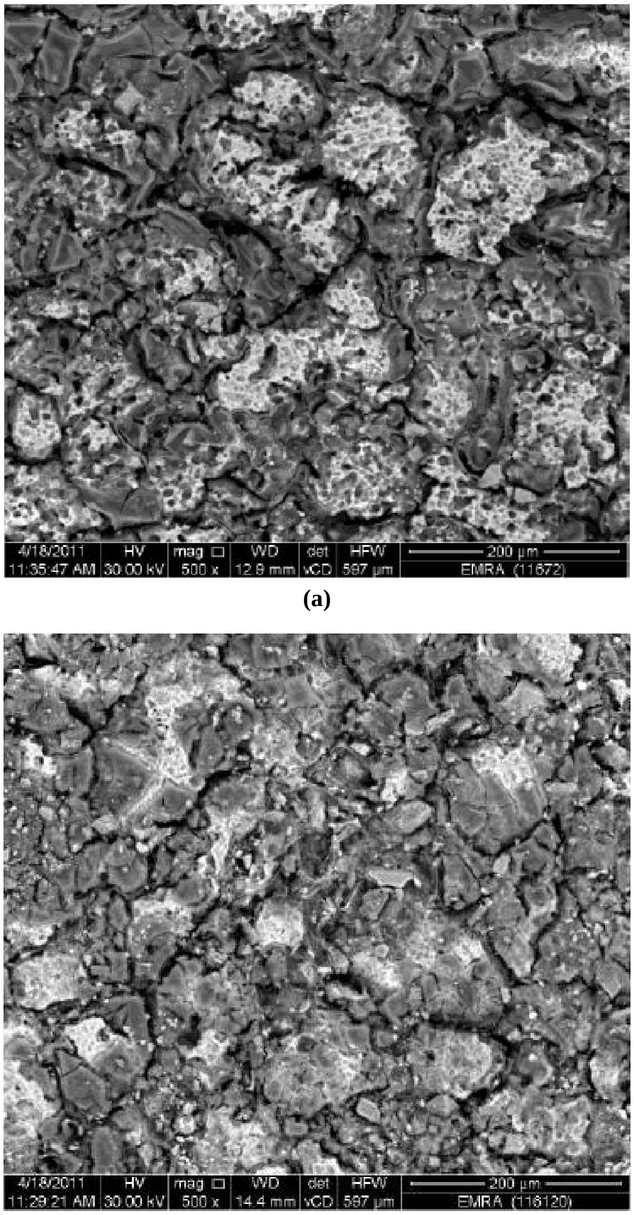

(a)

(b)

Figure 8 : FESEM micrographs of the corroded surfaces of Al/SiC nanocomposites containing 1 vol.-% of 200 nm SiC nanoparticles after exposure in 1 M HCl solution for 96 hr at (a) 50 and (b) 75 °C.

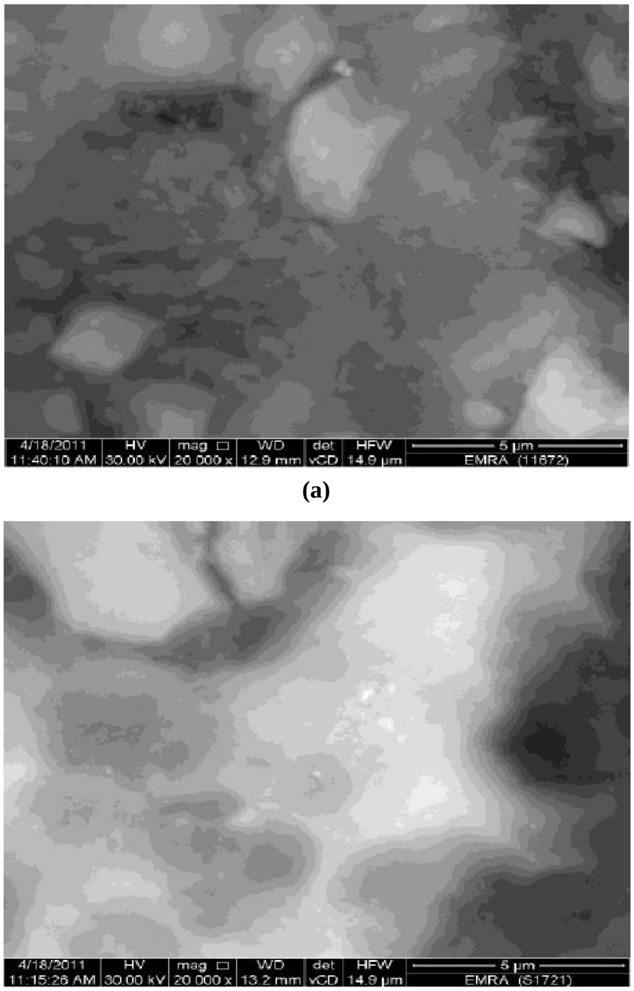

(a)

(b)

Figure 9 : High magnification FESEM micrographs for the corroded surfaces of Al/SiC nanocomposite specimens after exposure in 1 MHCl solution for 96 hr at 50 °C. (a) sample containing 1 vol.-% of 60 nm SiC nanoparticulates; (b) sample containing 1 vol.-% of 200 nm SiC nanoparticulates.

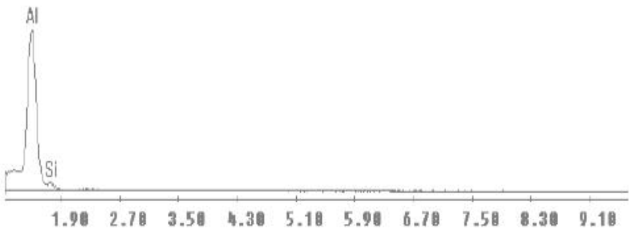

Figure 10 : EDX analysis of some SiC nanoparticles located at the grain boundaries.

nanoparticulates compared to that in the matrix metal. There is the evidence for the presence of grain boundary corrosion and pitting corrosion in the nanocomposites. This supports the effects of reinforcing nano-size SiC and Al_2O_3 nanoparticles in improving the corrosion resistance of the nanocomposites. The SiC and Al_2O_3 nanoparticles resist the severity of the acid attack to a certain extent. It is important to mention that there is hardly any information available in the literature about the corrosion behavior of the nanocomposites in acidic media.

CONCLUSIONS

According the results obtained from the current investigation, the following conclusions can be pointed out:

1. Both Al/SiC and Al/Al_2O_3 nanocomposites exhibited lower corrosion rates in 1 M HCl solution than the pure Al matrix. Such behavior was noticed at room temperature, 50 °C and 75 °C.
2. The Al/Al_2O_3 nanocomposites exhibited lower corrosion rates in 1 M HCl solution than the Al/SiC nanocomposites. The Al/Al_2O_3 containing (60 nm) exhibited the higher corrosion resistance among all the investigated nanocomposites.
3. The corrosion rate of the Al/SiC and Al/Al_2O_3 nanocomposites in 1 M HCl solution was reduced with the increase the exposure time and the volume fraction of the nanoparticles. While it increases with increasing the nanoparticles size and the solution temperature.

ACKNOWLEDGMENT

This work is supported by the King Abdel-Aziz City of Science and Technology (KACST) through the Science and Technology Center at King Khalid University (KKU), Fund (NAN 08-173-07). The authors thank both KACST and KKU for their financial support. Special Thanks to Prof. Dr. Ahmed Taher, Vice President of KKU, Prof. Dr. Eid Al-Atibi, Dean of the Scientific Research at KKU, and Dr. Khaled Al-Zailaie, Dean of the faculty of engineering at KKU, for their support.

REFERENCES

[1] ASM Handbook; Composites, **21**, **(2001)**.

[2] R.C.Paciej, V.S.Agarwala; Metallurgical variables influencing the corrosion susceptibility of a powder metallurgy aluminum/SiC_w composite, Corrosion, **42(12)**, 718-729 **(1986)**.

[3] Yoshiaki Shimizu, Toshiyasu Nishimura, Iwao Matsushima; ‘Corrosion resistance of Al-based metal matrix composites’, Mater.Sci.Eng.A, **198**, l l3-118 **(1995)**.

[4] Zhangsheng Liu, Bo Huang, Mingyuan Gu; ‘Corrosion behavior of Al/AlN_p composite in alkaline solution’, Materials Letters, **60**, 2024-2028 **(2006)**.

[5] I.S.El-Mahallawi, K.Eigenfield, F.Kouta, A.Hussein, T.S.Mahmoud, R.M.Ragaie, A.Y.Shash, W.Abou-Al-Hassan; Synthesis and characterization of new cast A356/$(Al_2O_3)_p$ metal matrix nano-composites’, ASME, In the proceeding of the 2nd Multifunctional nanocomposites & nanomaterials: International conference & exhibition, organized by the American University in Cairo - AUC, incollaboration with Cairo University, Sharm El Sheikh, Egypt, January 11-13, **(2008)**.

[6] T.G.Durai, Karabi Das, Siddhartha Das; Effect of mechanical milling on the corrosion behaviorof Al-Zn/Al_2O_3 composite in NaCl solution’, J.Mater.Sci., **42**, 8209-8214 **(2007)**.

[7] L.Bernad, (Ed); Hawk’s physiological chemistry, Oser, McGraw-Hill, TATA, 42 **(1976)**.

[8] ASTM G31-72 (Reapproved 2004); ‘Standard practice for laboratory immersion corrosion testing of metals, **(2004)**.

[9] JieLan, Yong Yang, Xiao Chun Li; ‘Microstructure and microhardness of SiC nanoparticles reinforced magnesium composites fabricated by ultrasonic method’, Materials Science and Engineering A, **386**, 284-290 **(2004)**.

[10] K.H.W.Seah, M.Krishna, V.T.Vijayalakshmi, J.Uchil; ‘Effects of the temperature and reinforcement content on corrosion characteristics of LM13/albite composites’, Corrosion Science, **44**, 7 **(2002)**.